Active source imaging from Newell County geologic carbon storage facility using a sparse network of SADAR arrays

Derek Quigley[1], Kevin D. Hutchenson[1,2], Paul A. Nyffenegger[1,2], and Mike Dahl[3]

[1]Quantum Technology Sciences, Inc. (Quantum); [2]Geospace Technologies, Inc.,[3]Geospace Technologies Canada, Inc.

Summary

In November 2021, Quantum Technology Sciences Inc. (Quantum) installed a sparse network of four permanent compact volumetric phased arrays (SADAR arrays) at Carbon Management Canada's Newell County Field Research Station (FRS). The FRS is a small-scale, experimental carbon sequestration site for testing reservoir measurement and monitoring technologies (Lawton *et al.*, 2019; Macquet *et al.*, 2022). The SADAR network has been used for ongoing passive microseismic event monitoring at the site (Hutchenson *et al.*, 2023, Hutchenson *et al.,* 2025; Nyffenegger *et al.*, 2025) and has recorded routine active-source vertical seismic profiling (VSP) time-lapse surveys conducted by Carbon Management Canada (Macquet *et al.*, 2022). These surveys are part of ongoing tests at the FRS site to monitor controlled volumes of CO_2 injected into the Basal Belly River Sandstone (BBRS, z=300 m) (Lawton *et al.*, 2019). In addition, the SADAR arrays are well-suited to record and process the active-source seismic survey data and monitor the reservoir across the midpoints between the survey lines and arrays. In this study, we present results from processing the seismic data recorded by the SADAR array network during ongoing active source seismic monitoring tests.

Introduction

Common and traditional methods to monitor small magnitude seismicity, or microseismicity, and man-made seismic events use passive surface or downhole sensors. However, the effectiveness of monitoring geologic carbon storage (GCS) operations with standard shallowly buried surface sensors may be limited due to a low signal-to-noise ratio for microseismic events even though they may cover a wide spatial area. In addition, most downhole sensor string use existing boreholes owing to the expense of drilling just for monitoring purposes, deploying sensors outside of the casing at some range of depths. As such, downhole instruments may offer limited coverage of the area of review (Eaton, 2018, 136), providing only limited views of the reservoir around the borehole. Furthermore, coverage of large areal extents using multiple instrumented boreholes dedicated to monitoring is financially unsupportable.

Our approach to monitor microseismicity is to deploy compact phased arrays (Nyffenegger *et al.*, 2025; Nyffenegger *et al.*, 2023, Zhang *et al.*, 2023; Nyffenegger *et al.*, 2022) below the weathering zone at an economic depth to drill and emplace equipment. Two dimensional (planar) arrays have been deployed for many years as an aid to global and regional monitoring, effective for exploiting the longer wavelengths associated with large events (Rost and Thomas, 2002). Quantum developed and successfully fielded compact volumetric phased arrays, permanently deployed at shallow depths but below the weathering layer. These SADAR arrays are designed for the higher frequencies and short wavelengths acquired at local scales and work especially well for microseismic applications.

A recent application is the inclusion of a sparse network of SADAR arrays to monitor the microseismicity at the FRS in Newell County, Alberta, for Carbon Management Canada (CMC).

The FRS was constructed to provide a methodological approach to CO_2 injection, capture, migration exploration, and as a test and proving ground for technologies to be investigated for measurement, monitoring, and verification (MMV) (Nyffenegger *et al.*, 2025; Lawton *et al.,* 2019).

In addition to passive detection and location of microseismicity, the arrays bring the ability to image geologic structure using active-source seismic surveys. Several vibroseis survey lines designed for vertical seismic profiles (VSP) have been completed since installation of the SADAR arrays. CMC periodically surveys the FRS to provide time-lapse VSP images using the downhole geophone string and distributed acoustic sensor (DAS) fiber installed in observation well #2 (Macquet *et al.*, 2022), a common approach. Generally though, because the VSP method is limited in its ability to image outward from the borehole, any substantial GCS plume will require constructing and instrumenting additional boreholes, or else augmenting the VSP with temporary surface geophone carpets, for obtaining more complete reservoir images. In contrast, the permanent SADAR arrays provide an effective and economical alternative to temporary repeated surface geophone deployments or permanently instrumenting additional boreholes, providing excellent imaging data for specific areas of concern, and informing a decision on if and when to perform a more extensive 3D survey.

Background

Four SADAR arrays were installed in mid-November of 2021 at distances between 70 m and 300 m from the injection site forming a sparse network (Figure 1). Since that time, they have been continuously operating (98.7% availability), recording seismic signals from microseismic events associated with or resulting from GCS processes. In addition, many events are recorded related to site activity at the surface, both within the compound and in the neighboring area. The SADAR arrays apply spatially coherent processing to produce three-dimensional beams that suppresses non-coherent noise and coherent noise from directions other than the beam main response axis (MRA), defined by the angle of arrival and the phase velocity at the array.

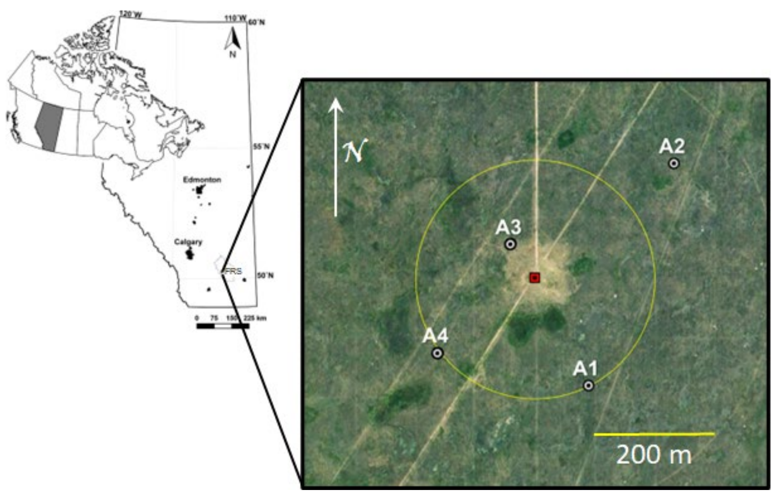

Figure 1. Canada with the location of the CMC FRS in Newell County and the array positions with respect to the injection well (red square). The arrays are located at 70 m (A3), 200 m (A1 and A4), and 300 m from the injection well (A2).

The physical layout of the arrays has been previously reported (Nyffenegger *et al.*, 2022, Zhang *et al.*, 2023). As shown in Figure 2, three array designs using Geospace GS-ONE 10 Hz vertical geophones were installed as uniform circular arrays (UCAs) at depths from 9 m-19 m:

1. a standard design consists of a 54-element, six layer octagonal UCA, and a central column,
2. a wide-aperture design consists of 51 elements, three layers, and a hexagonal UCA with a central column within a larger horizontal-aperture decagonal UCA for a total of 17 boreholes, and
3. a hybrid design consists of a 72-element array arranged as a hexagonal six-layer UCA with a central column within a larger wider-aperture decagonal three-layer UCA.

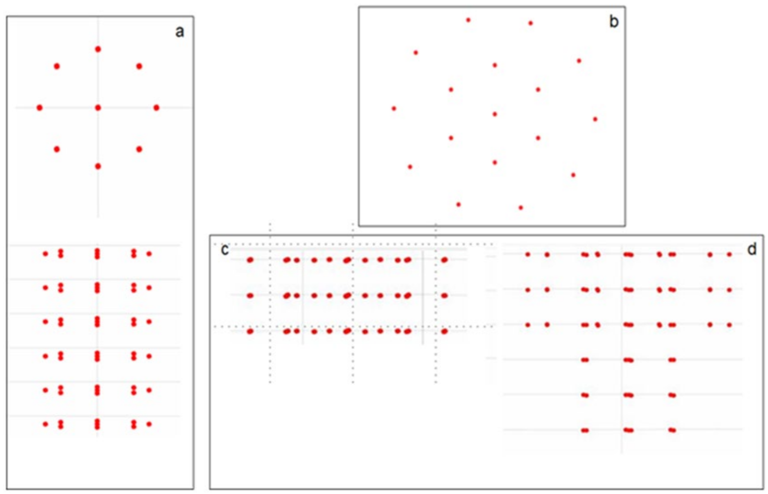

Figure 2. Layout of the installed and modeled arrays. (a) Standard octagonal UCA design with six layers (A1 and A2). Map view is shown at the top, and depth cross section at the bottom. (b) Map view of the wide-aperture and hybrid array designs with 17 boreholes in a nested UCA pattern. (c) Depth cross section for the wide-aperture layout with three layers (A3). (d) Depth cross section for the hybrid layout (A4). For A4, the outer decagonal UCA has three layers, and the hexagonal inner UCA and central column has six layers (Zhang *et al.*, 2023).

The arrays are designed with the elements along the UCA perimeters at half-wavelength spacing for an incident horizontal wavefront at the design frequency. For example, for an element spacing of 2 m, the frequency that corresponds to the wavelength (4 m) at the specified phase velocity (800 m/s) across the array is defined as the array design frequency (200 Hz). The volumetric array design provides a complete 3D sampling of the propagating wavefield across the array. The 3D sampling enables coherent array processing techniques to suppress noise and separate signals with different propagation parameters and provides a direct measurement of phase arrival angles and velocities (Nyffenegger *et al.*, 2023; Zhang *et al.*, 2023). The areal extent covered by the four SADAR arrays is approximately 150 m^2.

Since 2021, nearly 10,000 events have been located and vetted by a human analyst (Figure 3) using data acquired by the SADAR sparse network and a semi-automated processing pipeline (Hutchenson *et al.*, 2023). Ignoring the near surface events, 1522 events have been detected and located at depths exceeding 15 m using all four arrays. A fully automated near-real time processing pipeline was demonstrated at a recent GHGT-17 Conference field demonstration at the FRS site in October 2024.

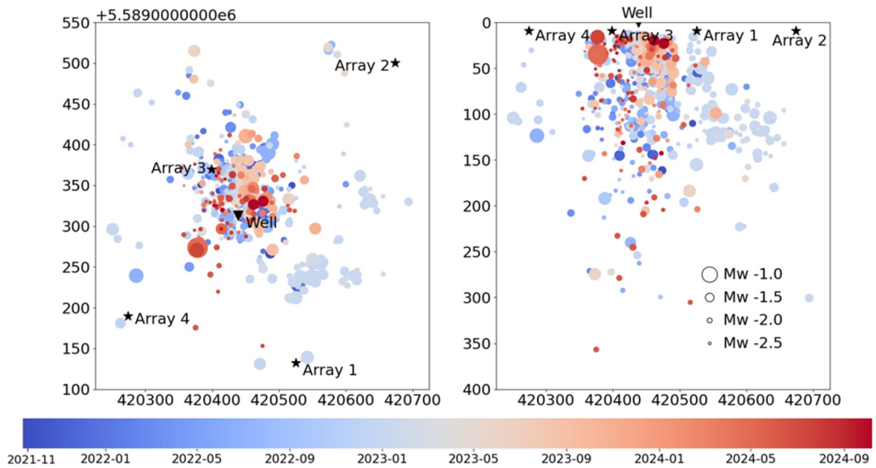

Figure 3. Location of 1522 events from November 2021 through October 2024 detected by all four (4) SADAR arrays with depths greater than 15 m. For this same time period, there were 9878 events if the shallow events are included (0 ≤ depth ≤ 15 m).

Furthermore, two repeatedly acquired survey lines (Lines 13 and 15), shown with respect to the SADAR arrays in Figure 4, are particularly well situated for generating optimum offset images using the SADAR arrays (Hunter and Pullan, 1989). The midpoints of the seismic lines between each of the arrays and the respective survey lines indicate the sampled reservoir area restricted to specular reflections from the survey shot points.

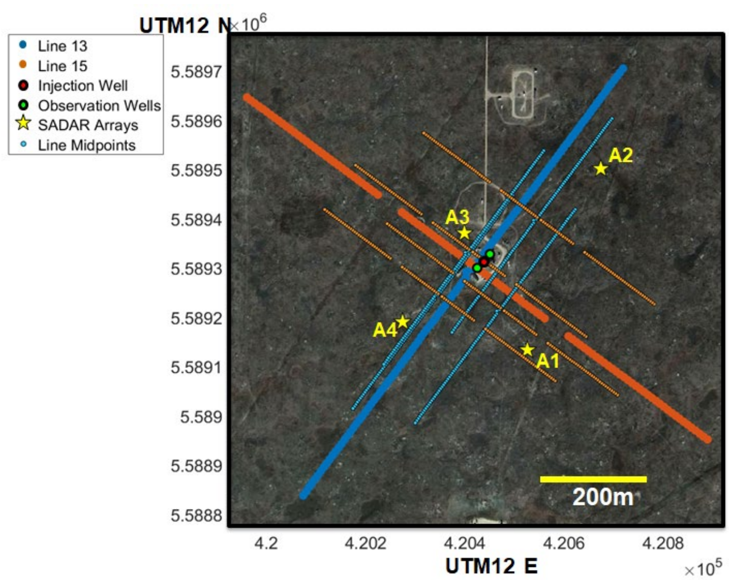

Figure 4. The location and length of the two survey (Vibroseis) lines (thick lines). The thinner, dotted lines represent the midpoint sections at the reservoir each of the respective arrays sample with specular reflections.

Method

The two recent survey lines listed in Table 1 were conducted in October 2024 and are periodically repeated several times a year. Shots recorded by the SADAR passive permanent monitoring network are extracted from the continuously recorded time series at times corresponding to the known survey shot times. The monitor survey lines were acquired using typical vibroseis units which record GPS of the shot positions for repeatability. The Envirovibe source used with this survey is owned and operated by the University of Calgary and configured for a 10-150 Hz, 16 second linear sweep (Figure 5).

Table 1. Summary of survey lines from October 2024.

Survey Date	Survey Lines	N Shot Stations	Shot Station Fold
October 2024	13	109	4
October 2024	15	106	4

Figure 5. The University of Calgary Envirovibe vehicle.

Data shot segments are processed in a conventional seismic reflection processing sequence with the addition of beamforming. The processing sequence for the monitor survey lines includes:

1) Cross correlation of shot segments with the known vibroseis sweep.
2) Averaging repeat shots from the same stations on the same survey dates.
3) Beamforming the arrays to a specific depth point.
4) Sorting common receiver gathers to form a representative subsurface cross-section.
5) Normal moveout (NMO) correction, data scaling, and other enhancement.

Beamforming data from the arrays, as used for this demonstration, targets specular reflections from a depth horizon arriving at the array with a specific angle, for survey line source midpoints, producing one beam per shot point. The targeted beam is formed by applying time shifts to the individual array sensors prior to averaging, or stacking, the array data, aligning coherent wavefronts at the chosen angle of arrival. In this case, reflection points were chosen at the Medicine Hat formation depth as a compromise, because it is expected that angle of arrival will be sufficient to improve imaging for the BBRS as well as the Manville group, owing to the width of the beam main lobe.

It is also possible to assemble a composite beam for each midpoint from multiple targeted beams simply by windowing the individual beams and summing across the set. Other standard array signal processing operations can be applied, for example, to null energy from undesired directions or sources. However, simple targeted beam images are shown here to demonstrate the effectiveness of the SADAR arrays and the method.

Beamforming shift factors are computed deterministically by ray tracing a 1D depth velocity model based on the sonic log from well #2 from each targeted depth point to the array element positions defining a beam MRA, and then including the travel time differences between the element positions and a reference position at the centroid of each array. For example, considering deep reflections with narrow incidence angles, the MRA is near vertical, and the beam can be thought of primarily as a static shift to align the multi-levels of the SADAR array.

The results from two lines shot in October 2024 (Figure 6 through Figure 9), illustrate the image quality produced from the SADAR arrays and targeted beamforming. The midpoint profile calculated between Line 13 and all four arrays is shown in Figure 6 and Figure 7, and for Line 15 and all four arrays is shown in Figure 8 and Figure 9.

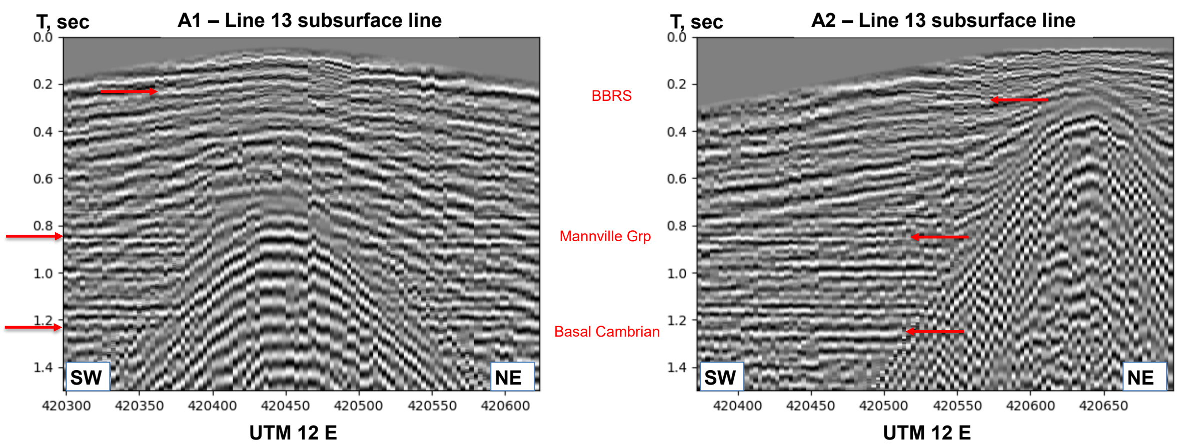

Figure 6. Seismic cross-section profiles calculated from the October 2024 survey, Line 13, A1 and A2. Horizontal axis is UTM East midpoint location.

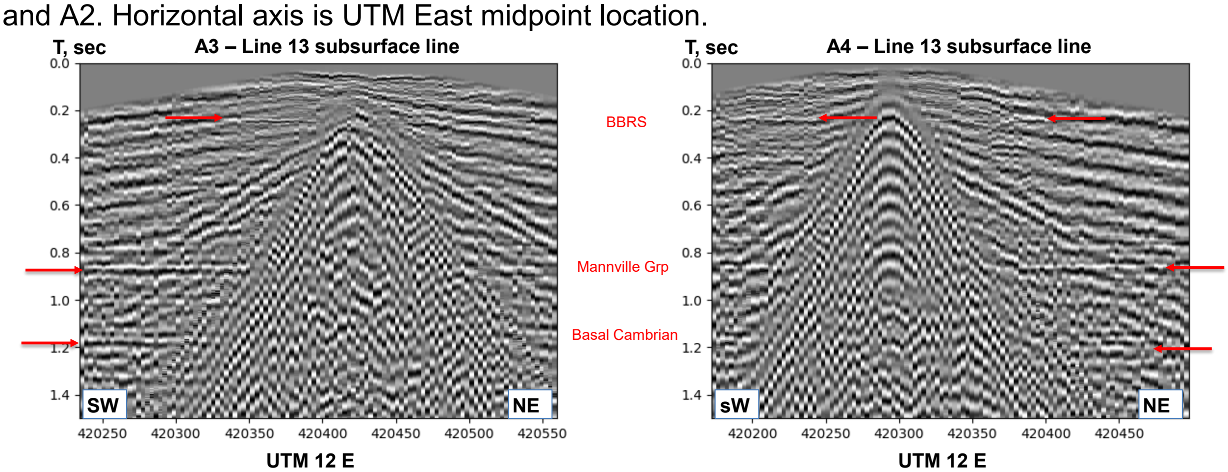

Figure 7. Seismic cross-section profiles calculated from the October 2024 survey, Line 13, A3 and A4. Horizontal axis is UTM East midpoint location.

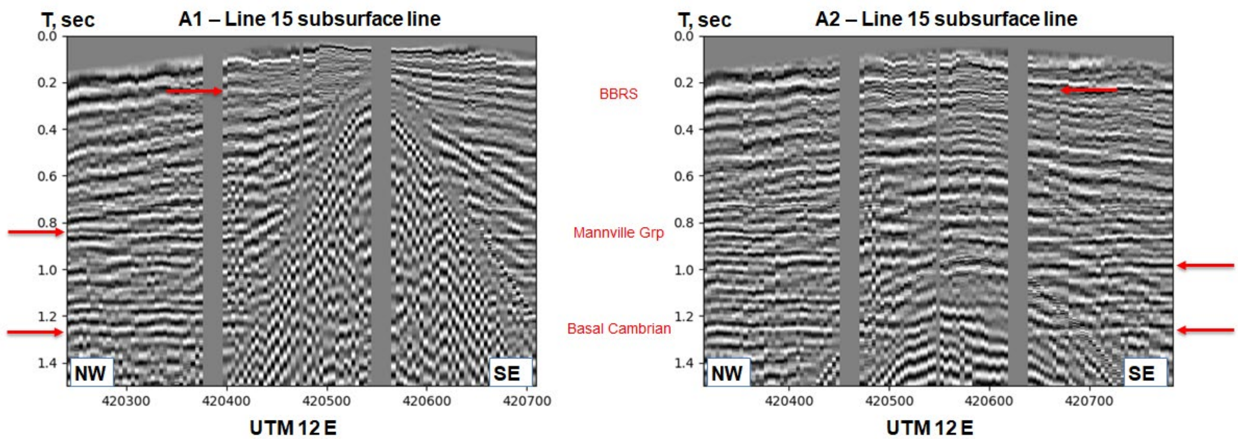

Figure 8. Seismic cross-section profiles calculated from the October 2024 survey, Line 15, A1 and A2. Horizontal axis is UTM East midpoint location. Gaps indicate no-data zones due to pipeline infrastructure.

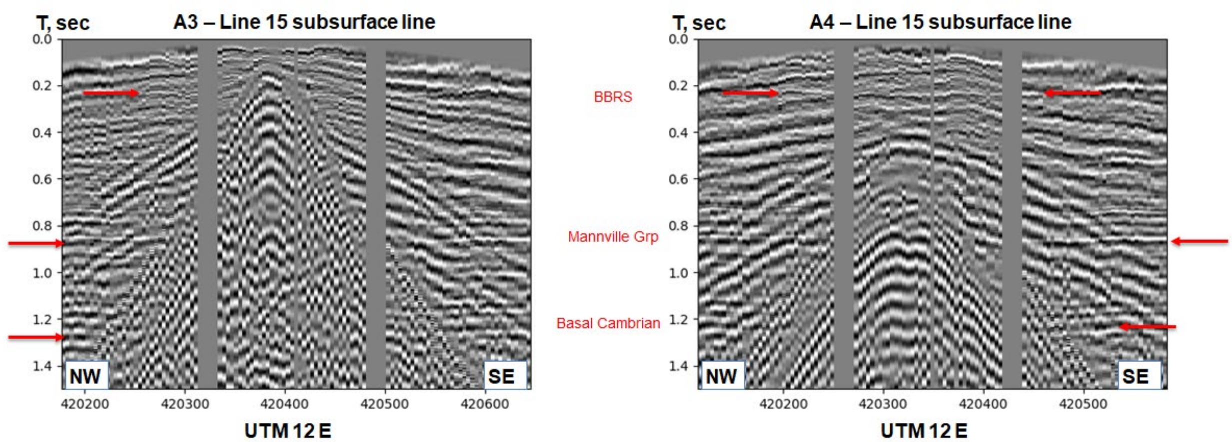

Figure 9. Seismic cross-section profiles calculated from the October 2024 survey, Line 15, A3 and A4. Horizontal axis is UTM East midpoint location. Gaps indicate no-data zones due to pipeline infrastructure.

The Basal Belly River Sandstone (BBRS), the unit in which CO_2 injection is occurring, is clearly visible in the images at approximately 0.25 seconds two-way travel time. The BBRS typically falls in an optimal offset window outside of the surface wave noise cone (Hunter and Pullan, 1989). The reflectors associated with the Lower Mannville Group (0.85 seconds) is also clearly resolved and over a greater areal extent than the shallower BBRS unit. Even the bottom of the Cambrian sediments, and top of the Precambrian basement at approximately 1.2 seconds of two-way travel time, or 1500-1800 m (Burwash *et al.*, 1994) is resolved.

Zooming on the profile for Line 13 at A3 in Figure 10, the enhanced results from targeted beamforming (right) are compared with the single sensor receiver gather (left). There is a marked improvement in resolving the BBRS and the Mannville Group strata; both the vertical delineation of the bed and the horizontal continuity is improved in the profile as the coherent air wave/ ground roll noise is suppressed.

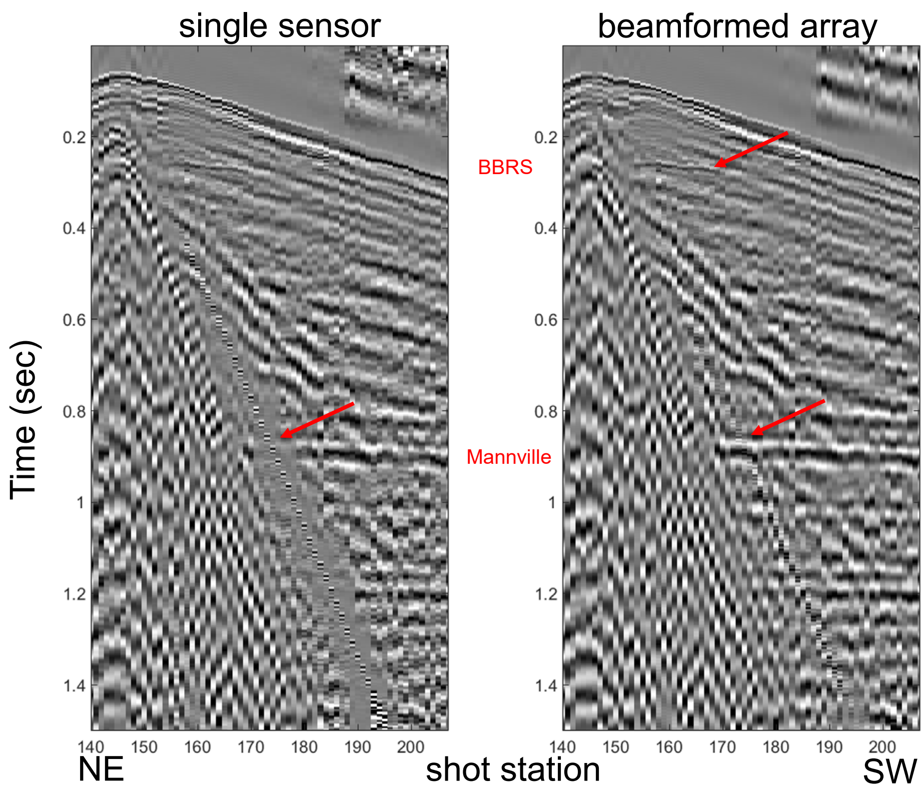

Figure 10. Seismic cross section subset from the October 2024 monitor survey for the A3 - Line 13 subsurface line showing both the reference sensor (center platter middle sensor) (left) and the targeted beam (right). Note the improvement in the BBRS horizon and the Mannville Group by beamforming to those depth points, increasing the definition and continuity of these features.

Conclusions

This study illustrates the dual capability of SADAR arrays. Their depth of burial improves the SNR by an emplacement that eliminates much of the surface generated noise (Eaton, 2018). The SNR is further enhanced using coherent beams to suppress both non-coherent noise and coherent noise arriving at angles off the MRA and at different phase velocities. This basic phased array capability enables maximizing the received signal SNR for both the passive microseismic monitoring and active-source survey applications. Previous studies demonstrated the robustness of the arrays to perform with missing sensors for both passive monitoring and active-source surveys (Hutchenson *et al.*, 2025; Quigley *et al.,* 2025). Nevertheless, the array hardware is engineered for a persistent and permanent presence and has been operating for over 3 years at nearly a 99% availability. The SADAR array sparse network has allowed the detection and location of nearly 10,000 events with magnitude ranges from approximately -0.5 Mw down to -2.75 Mw over a three-year period (Hutchenson *et al.*, 2025; Hutchenson *et al.,* 2023).

Furthermore, this study demonstrates at an active GCS site the dual-use capability of permanently emplaced SADAR phased arrays for enhanced active-source seismic reflection imaging of targeted geologic volumes. By beamforming the elements of each array to a targeted depth, the SNR of the signal and image improves beyond standard seismic profiling. Coherent noise arriving outside the MRA lobe such as the air wave and ground roll is suppressed as illustrated in Figure 10, extending the optimum offset window (Nyffenegger *et al.*, 2025). Altogether, with the enhanced processing and dual use capability of SADAR arrays, the small areal extent, and the robust design and system components, seismic MMV using SADAR systems provides a single permanently emplaced system that guarantees ability of monitoring geologic assets using both passive and active source methods.

Acknowledgements

Quantum Technology Sciences, Inc., is a wholly owned subsidiary of Geospace Technologies Corporation, Inc. We acknowledge CMC for providing access to the CaMI Newell County Facility to enable installation of the SADAR system, and for sharing the data from the surface and downhole networks. The Newell County Facility is supported by funding from the Global Research Initiative at the University of Calgary from the Canada First Research Excellence Fund and from the CaMI Joint Industry Project. CMC is also acknowledged for providing operational data from the site. We especially thank Marie Macquet and the CMC staff for extending the vibroseis lines in October to increase the midpoint extents.

References

Burwash, R.A., C.R. McGregor, and J. Wilson ,1994, Ch. 5, Precambrian basement beneath the Western Canada Sedimentary Basin, *in* Geological Atlas of the Western Canada Sedimentary Basin, G.D. Mossop and I. Shetsen (comp.), Canadian Society of Petroleum Geologists and Alberta Research Council, URL https://ags.aer.ca/atlas-the-western-canada-sedimentary-basin/chapter-5-Precambrian-basement.

Eaton, D.W., 2018, Passive seismic monitoring of induced seismicity: fundamental principles and application to energy technologies: Cambridge University Press, 30 pp.

Hunter, J.A., and S.E. Pullan, 1989, The optimum offset shallow seismic reflection technique: Proceedings of the Symposium on the Application of Geophysics to Engineering and Environmental Problems, EEGS, 143-174.

Hutchenson, K.D., J. Jennings, E.B. Grant, D. Quigley, J. Yelton, and P.A. Nyffenegger, 2025, Persistent microseismic monitoring using robust permanent SADAR arrays: to be presented at CCUS, Houston, 3-5 March 2025.

Hutchenson, K.D., D. Quigley, J. Longbow, E.B. Grant, P.A. Nyffenegger, J. Jennings, M.A. Tinker, M. Dahl, D. Grindell, M. Macquet, and D.C. Lawton, 2023, Microseismic monitoring using SADAR arrays at the Newell County carbon storage facility: what have we learned in a year?: presented at Geoconvention, 2023, Calgary.

Lawton, D.C., J. Dongas, K. Osadetz, A. Saeedfar, and M. Macquet, 2019, Chapter 16: Development and analysis of a geostatic model for shallow CO2 injection at the Field Research Station, Southern Alberta, Canada, *in* T. Davis, M. Landro, and M. Wilson, eds., Geophysics and Geosequestration: Cambridge University Press, 280-296, doi.org/10.1017/9781316480724.017.

Macquet, M., D. Lawton, K. Osadetz, G. Maidment, M. Bertram, K. Hall, B. Kolkman-Quinn, J. Monsegny Parra, F. Race, G. Savard, and Y. Wang, 2022, Overview of Carbon Management Canada's pilotscale CO2 injection site for developing and testing monitoring technologies for carbon capture and storage, and methane detection: Recorder Focus Article, **47**(1), April 2022.

Nyffenegger, P.A., D.C. Lawton, M. Macquet, D. Quigley, B. Kolkman-Quinn, and K.D. Hutchenson, 2025, Advances in coupled passive and active seismic monitoring for large-scale geologic carbon storage projects, *in* Wilson, M., T. Davis, and M. Landro, eds., Geophysics and the Energy Transition: Elsevier Press, 333-354.

Nyffenegger, P.A., J. Zhang, E.B. Grant, D. Quigley, K.D. Hutchenson, M.A. Tinker, D.C. Lawton, and M. Macquet, 2023, Performance and outlook for SADAR array network at the Newell County Facility: First Break, **41**, 56-62.

Nyffenegger, P.A., M.A. Tinker, J. Zhang, E.B. Grant, K.D. Hutchenson, and D.C. Lawton, 2022, Compact phased arrays for microseismic monitoring: First Break, **40**, 69-74.

Quigley, D., P.A. Nyffenegger, K.D. Hutchenson, and J. Yelton, 2025, Active source sparse imaging using permanent SADAR arrays; to be presented at CCUS, Houston, 3-5 March 2025.

Rost, S. and C. Thomas, 2002, Array seismology: methods and applications: Rev. Geophys., 40(3), 2.1-2.27.

Zhang, J., K.D. Hutchenson, P.A. Nyffenegger, E.B. Grant, J. Jennings, M. Tinker, M. Macquet, and D.C. Lawton, 2023. Performance comparison of compact phased arrays and traditional seismic networks for microseismic monitoring at a CO_2 sequestration test site: The Leading Edge, **42**(5), 332-342.